A novel plant toxin, persin, with *in vivo* activity in the mammary gland, induces Bim-dependent apoptosis in human breast cancer cells

Alison J. Butt,[1,2] Caroline G. Roberts,[1]
Alan A. Seawright,[3] Peter B. Oelrichs,[3]
John K. MacLeod,[4] Tracy Y.E. Liaw,[5]
Maria Kavallaris,[5] Tiffany J. Somers-Edgar,[1]
Gillian M. Lehrbach,[1] Colin K. Watts,[1]
and Robert L. Sutherland[1,2]

[1]Cancer Research Program, Garvan Institute of Medical Research, St. Vincent's Hospital, Darlinghurst, New South Wales, Australia; [2]St. Vincent's Clinical School, Faculty of Medicine, University of New South Wales, Sydney, New South Wales, Australia; [3]National Research Centre for Environmental Toxicology, University of Queensland, Brisbane, Queensland, Australia; [4]Research School of Chemistry, Australian National University, Canberra, Australian Capital Territory, Australia; and [5]Children's Cancer Institute Australia for Medical Research, Randwick, New South Wales, Australia

Abstract

Phytochemicals have provided an abundant and effective source of therapeutics for the treatment of cancer. Here we describe the characterization of a novel plant toxin, persin, with *in vivo* activity in the mammary gland and a p53-, estrogen receptor –, and Bcl-2-independent mode of action. Persin was previously identified from avocado leaves as the toxic principle responsible for mammary gland – specific necrosis and apoptosis in lactating livestock. Here we used a lactating mouse model to confirm that persin has a similar cytotoxicity for the lactating mammary epithelium. Further *in vitro* studies in a panel of human breast cancer cell lines show that persin selectively induces a G_2-M cell cycle arrest and caspase-dependent apoptosis in sensitive cells. The latter is dependent on expression of the BH3-only protein Bim. Bim is a sensor of cytoskeletal integrity, and there is evidence that persin acts as a microtubule-stabilizing agent. Due to the

unique structure of the compound, persin could represent a novel class of microtubule-targeting agent with potential specificity for breast cancers. [Mol Cancer Ther 2006;5(9):2300–9]

Introduction

Breast cancer is the leading cause of cancer death amongst women in developed countries. Despite increased understanding of the molecular aberrations underlying this disease and advances in detection and treatment, intrinsic or acquired therapeutic resistance remains a major obstacle to an effective cure (1), emphasizing the need for the development of novel molecular and pharmacologic therapeutics with increased selectivity and efficacy. To this end, much attention has focused on the chemotherapeutic properties of plant chemicals, some of the most widely used being the microtubule poisons, taxanes, that include paclitaxel and its derivatives, which have antitumor activity against a range of human cancers, including those of the breast and ovary (2). This class of drug mediates its effects by directly interacting with the microtubules. More recently, several structurally unrelated classes of microtubule-interacting agents have been discovered and characterized (reviewed in ref. 3), emphasizing the importance of the intracellular cytoskeleton as a target for anticancer agents.

It has previously been noted that lactating livestock develop a noninfectious mastitis and loss of milk production after eating avocado (*Persea americana*) leaves. This effect is associated with a specific necrosis of the secretory epithelium of the mammary gland (4). Similar results were observed in lactating mice fed freeze-dried avocado leaves (5), and this model led to the isolation of the active agent, persin [(+)-(Z,Z)-1-(acetyloxy)-2-hydroxy-12,15-heneicosadien-4-one; Fig. 1; ref. 6]. Enantioselective syntheses of the *R* and *S* enantiomers of persin showed only the *R* enantiomers active in the range of 60 to 100 mg/kg body weight. Only at high doses of persin (>100 mg/kg) are other tissues (e.g., myocardium) affected (6). Interestingly, the necrotic effect of persin in the mammary gland is cumulative, but the effect on myocardial fibers is not. This apparent activity in the mammary gland suggests that persin could be developed as a novel therapy for breast cancer.

Persin is synthesized in idioblast oil cells present in avocado fruit and leaves and is thought to function as a natural insecticide and fungicide (reviewed in ref. 7). Avocado acetogenins, such as persin, are derived from the biosynthesis of long-chain fatty acids, and persin itself is the deoxy-derivative of glyceride, with close structural homology to the monoglyceride of linoleic acid.
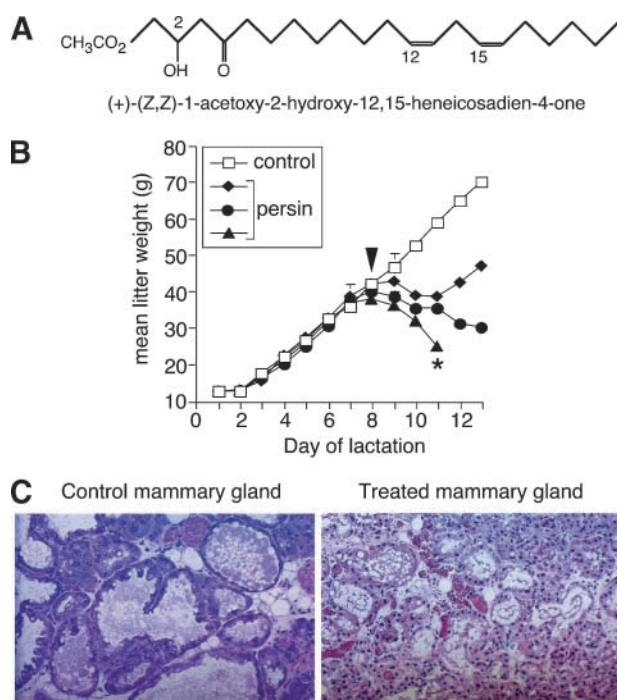
Figure 1. Mammary-specific effects of persin *in vivo*. **A**, chemical structure of persin. **B**, mean pup weights (± SE) for three persin-treated and one control litter after a single exposure of lactating mice to persin (*arrow*). *, litter died of starvation. Where error bars are not shown, they did not exceed the size of the respective symbols. **C**, representative photomicrographs showing H&E staining of mammary epithelium from normal lactating dam and dam treated with single dose of persin. Magnification ×250.

Interestingly, conjugated linoleic acid has received some attention as an anticarcinogenic agent with particular efficacy against breast cancer (8). There is also some evidence that polyunsaturated fatty acids can enhance the sensitivity of breast cancer cells to chemotherapeutic agents, such as paclitaxel (9).

Here we have examined both the cytostatic and cytotoxic effects of persin in breast cancer cell lines and determined its effects on key regulators of these processes. Persin-induced apoptosis is associated with specific changes to the microtubules. Furthermore, persin induces apoptosis in human breast cancer cells lines independently of the p53, estrogen receptor, and Bcl-2 status of the cells. These data provide support for the further development of persin as a novel chemotherapeutic with potential efficacy against refractory breast cancers.

Materials and Methods

Purification and Isolation of Persin

The isolation and purification of persin from milled freeze-dried leaves of the avocado, *P. americana*, has previously been described (6). The purity of batches used in the present study was monitored by proton magnetic resonance at 300 MHz in CDCl3 with a Varian Gemini NMR Spectrometer, and by measurement of its optical rotation, $[\alpha]_D^{22}$ +11.98 (c = 10.0 mg/mL in CHCl$_3$), with a Perkin-Elmer model 241 spectropolarimeter as previously described (6).

Experimental Intoxication in the Mouse

Studies were carried out in Quackenbush mice on their first lactation. Persin (100 mg/kg) was delivered as an aqueous suspension by gavage as a single dose to mice on the 8th day of lactation (*arrow*), by which time milk production is considered maximal. Pup body weight was measured daily after dosing and used as an indirect indicator of mammary gland function and milk production. Apart from a transient period of weight loss lasting 24 hours, persin treatment was normally without overt harmful effect on the dam. All experiments were carried out with the approval of the Institutional Animal Care and Ethics Committee.

Cell Culture of Breast Cancer Cells

The human breast cancer cell lines MDA-MB-231, MCF-7, and T-47D were routinely maintained in RPMI 1640 supplemented with 10% FCS, 10 μg/mL insulin, and 2.92 mg/mL glutamine under standard conditions.

Stable Transfection

MCF-7 and T-47D cells were stably transfected with human Bcl-2 cDNA in the expression vector pEF (a kind gift from Dr. David Huang, The Walter and Eliza Hall Institute of Medical Research, Australia) using Fugene (Invitrogen Life Technologies, Inc., Carlsbad, CA) according to the protocol of the manufacturer. Stably expressing clones were selected and grown up for further experiments.

Cell Proliferation Assays

Cells were treated with concentrations of persin or vehicle in 10% FCS medium. On days 1, 2, 3, and 6 of treatment, cells were trypsinized and the viable cell number was determined by trypan blue exclusion and cell counting.

Survival Assays

The long-term survival of breast cancer cells following 2 hours of treatment with persin was assessed by survival assay as previously described (10).

Measurement of Apoptosis by Flow Cytometry

Cells were incubated for 24 hours with the caspase-8-specific inhibitor z-IETD-fmk or the caspase-9-specific inhibitor z-LEHD-fmk (both 20 μmol/L; BD PharMingen, San Diego, CA) or vehicle control. For pre-G$_1$ analysis, floating and attached cell populations were prepared as previously described (10) and flow cytometric analysis was done with a Coulter ELITE flow cytometer (Coulter, Hialeah, FL). For M30 analysis, floating and attached cell populations were combined, washed with PBS, fixed, and permeabilized in ice-cold methanol, then resuspended in PBS with FITC-conjugated M30 CytoDEATH monoclonal antibody (1:100; Alexis Biochemicals, Lausen, Switzerland) before the M30-positive population was determined by flow cytometry. Caspase-9 activation was measured in floating and attached cells by flow cytometry after labeling with a carboxyfluorescein-labeled caspase-9 inhibitor, FAM-LETD-fmk (Kamiya Biomedical Company, Seattle, WA), following the instructions of the manufacturer.

Analysis of Cytochrome *c* and Smac/DIABLO Release

The release of cytochrome *c* and Smac/DIABLO from mitochondria was determined by immunoblotting of cytoplasmic extracts prepared essentially as previously described (11).

Tubulin Polymerization Assay

Soluble and polymerized fractions of tubulin were separated and quantitated as previously described (12).

Immunoblot Analysis

Proteins from whole-cell lysates were resolved under reducing conditions on 12% or 15% SDS-polyacrylamide gels using standard methods. Resolved proteins were transferred to nitrocellulose membranes and probed with antibodies against Bcl-2 (DakoCytomation, Glostrup, Denmark), Bax, Bad, Bak, Bcl-x_L, cyclin B1, cytochrome *c*, $p27^{KIP1}$, $p21^{WAF1/CIP1}$ (all BD PharMingen), Bim (Calbiochem, Darmstadt, Germany), cyclin D1 (Novacastra Laboratories Ltd., Newcastle upon Tyne, United Kingdom), phospho–c-jun NH_2-terminal kinase (JNK; Cell Signaling Technologies, Inc., Danvers, MA), total JNK, cyclin A, and Smac/DIABLO (Santa Cruz Biotechnology, Santa Cruz, CA), overnight at 4°C or for 2 hours at room temperature. Immunoreactive protein bands were detected by the relevant anti–immunoglobulin G antibodies conjugated with horseradish peroxidase followed by enhanced chemiluminescence (Pierce, Rockford, IL). Blots were checked for equal loading by reprobing with anti-actin antibody (Sigma, St. Louis, MO).

Immunofluorescence

Cells were seeded into chamber slides and treated with persin in the presence or absence of 20 μmol/L of caspase inhibitors, z-LEHD-fmk or z-IETD-fmk (BD PharMingen). Cells were briefly rinsed with PBS, then fixed with ice-cold 100% methanol at −20°C for 10 minutes. Fixed cells were then rinsed with PBS and blocked with 10% FCS/PBS for 10 minutes. Slides were incubated with α-tubulin antibody (Sigma) at 37°C for 30 minutes, then washed with PBS/0.1% Tween 20 at room temperature. Slides were incubated with antimouse/Cy2 conjugate and the nuclear dye 4,6-diamidino-2-phenylindole, and then visualized by confocal microscopy.

RNA Interference

Bim-specific small interfering RNA (siRNA) and non-targeting negative controls were purchased from Dharmacon, Inc. (Lafayette, CO). Cells were transfected with Lipofectamine 2000 (Invitrogen Life Technologies) in the presence of siRNAs according to the protocol of the manufacturer.

Statistical Analysis

Statistical analysis was carried out with StatView 4.02 (Abacus Concepts, Inc., Berkeley, CA). Differences between groups were evaluated by Fisher's protected least significant difference test after ANOVA using repeated measures or factorial analysis where appropriate.

Results

Persin Induces Pathologic Changes in the Mammary Gland of Lactating Mice

Figure 1B is a representative experiment of the effects of persin on the lactating mammary gland. Lactating Quack-

enbush mice were dosed with persin and the effect on the pup weight was used as an indirect indicator of mammary gland function. The volume of milk produced by dams treated with persin was significantly reduced compared with untreated dams, and any toxic effect experienced by the dam after an oral dose that affected the mammary glands only was usually transient and characterized by a moderate loss of body weight lasting no more than 24 hours.[6] Figure 1B illustrates that the pups of persin-treated dams had a reduced weight compared with untreated dams. In most dams necropsied at 48 hours post-dosing, the mammary glands were grossly swollen and hyperemic. Histologically, there were variable degrees of extensive necrosis and/or apoptosis of alveolar epithelium when compared with untreated controls (Fig. 1C). There were no visible signs of persin effects on other tissues examined.

Inhibition of Human Breast Cancer Cell Proliferation by Persin

MCF-7, T-47D (both estrogen receptor positive), and MDA-MB-231 (estrogen receptor negative) cells were treated with increasing concentrations of persin (6.9–27.6 μmol/L), then viable cell numbers were determined by trypan blue exclusion and cell counting. Figure 2A shows that both MCF-7 and T-47D cell proliferation were significantly inhibited at all the concentrations of persin ($P < 0.01$, repeated measures ANOVA) compared with control cells. MDA-MB-231 cells were relatively resistant to the cytostatic effects of persin compared with MCF-7 and T-47D, although significant growth inhibition was observed at concentrations of 27.6 μmol/L ($P < 0.01$, repeated measures ANOVA).

Induction of a G_2-M Cell Cycle Arrest by Persin

The effects of persin on cell cycle progression were examined by flow cytometry. Figure 2B shows the percentage of each cell population in the G_2-M phase of the cell cycle following 48 hours of treatment with persin. No significant changes in cell cycle progression were observed in treated MDA-MB-231 cells. However, treatment of MCF-7 and T-47D cells resulted in a significant accumulation of cells in G_2-M compared with untreated controls. We also observed a significant decrease in the percentage of MCF-7 and T-47D cells in S phase compared with untreated controls (data not shown), indicating the effects on G_1 to S phase progression in sensitive cells.

To further elucidate the mechanism of the cytostatic effects of persin, we determined the effects of persin treatment on a panel of proteins involved in cell cycle progression. Cells were treated with 27.6 μmol/L persin for 24 or 48 hours and whole-cell lysates were prepared for immunoblot analysis. Treatment of the sensitive cell lines MCF-7 and T-47D with persin resulted in a decrease in expression of the S-phase cyclin and cyclin A and the G_1-phase cyclin and cyclin D1 (Fig. 2C). This is consistent with our data showing a decrease in S phase

---

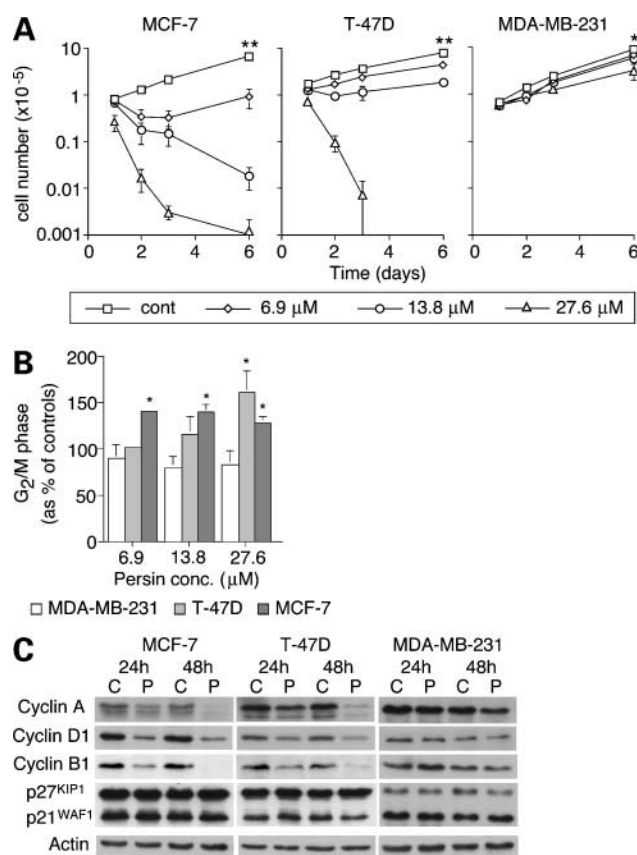[6] A.A. Seawright, personal communication.

Figure 2. Effect of persin on the proliferation of human breast cancer cell lines. **A,** cells were treated with persin as indicated and viable cell numbers determined on days 1, 2, 3, and 6 of treatment by trypan blue exclusion and cell counting. *Points,* mean of triplicate wells from at least two independent experiments; *bars,* SE. *, $P < 0.05$, persin-treated (10 μg/mL) cells versus untreated controls; **, $P < 0.001$, persin-treated cells versus untreated controls (repeated measures ANOVA). **B,** cells were treated with persin for 48 h, then fixed and stained with the DNA dye propidium iodide before flow cytometric analysis of cell cycle phase distribution. *Columns,* mean of cells from triplicate wells from three independent experiments expressed as percentage of untreated control cells; *bars,* SE. *, $P < 0.05$, persin-treated cells versus untreated controls. **C,** cells were treated with 27.6 μmol/L persin (*P*) or control (*C*) for 24 or 48 h as indicated, then whole-cell lysates were prepared and analyzed for expression of cell cycle regulatory proteins by immunoblot. Representative immunoblots from two independent experiments.

in persin-treated cells (data not shown). The MDA-MB-231 cell line also showed a decrease in expression of cyclin D1 and cyclin A after 48 hours of treatment, which is consistent with the cytostatic effects of persin at this dose in these cells (Fig. 2A). Cyclin B1 controls progression through G_2-M phase. Consistent with the observed arrest in G_2-M phase in sensitive cells, there was a decrease in cyclin B1 expression at both 24 and 48 hours after treatment of MCF-7 and T-47D cells. No significant changes were seen in MDA-MB-231 cells. We also observed no changes in expression of either of the cyclin-dependent kinase inhibitors p21[WAF1/CIP1/SDI1] or p27[KIP1] following persin treatment (Fig. 2C).

Persin Treatment Causes Bundling of Microtubules in Sensitive Cells

The G_2-M arrest seen in persin-treated cells is similar to that induced by a class of anticancer agents, termed microtubule stabilizers, such as paclitaxel. We examined the morphologic effects of persin exerted on cellular microtubules by indirect immunofluorescence and compared the microtubular architecture to that seen following paclitaxel treatment (Fig. 3A). Untreated cells exhibited microtubule arrays radiating from the center to the cell periphery, whereas persin-treated MCF-7 and T-47D cells exhibited microtubule networks reorganized into thick, peripheral bundles. This effect is similar to that seen following treatment with paclitaxel (Fig. 3A). Interestingly, whereas MDA-MB-231 cells were resistant to persin-induced microtubule changes, they did respond to paclitaxel treatment, suggesting that the compounds may have differing mechanisms of action or uptake kinetics. To exclude the possibility that the changes to microtubules in persin-treated cells are due to the rounding of cells during the apoptotic process, apoptosis was blocked using either z-IETD-fmk or z-LEHD-fmk. Persin treatment still resulted in microtubular bundling even when the apoptotic process was blocked (data not shown), suggesting that persin exerts direct effects on the microtubular architecture.

To further examine this hypothesis, we determined the effects of persin treatment on the polymerization of tubulin in MCF-7 cells. Figure 3B shows that treatment with either persin or paclitaxel resulted consistently in a significant increase in polymerized tubulin compared with untreated controls. Although the basal levels of polymerized tubulin observed in these cells under these conditions were relatively high, the effects of both persin and paclitaxel were maximal at the lowest doses examined.

Proapoptotic Effects of Persin in Breast Cancer Cells

We next examined the effects of persin on the long-term survival of human breast cancer cells using clonogenic assays. Figure 4A shows the survival of persin-treated cells compared with untreated controls. MDA-MB-231 cells were not significantly affected by persin treatment and no significantly decreased survival was observed in persin-treated cells compared with controls. However, persin treatment of MCF-7 and T-47D cells resulted in a significant decrease in survival compared with controls at all concentrations of persin examined (Fig. 4A). Comparable IC_{50} values for the three cells lines showed the relative resistance of MDA-MB-231 cells to the cytotoxic effects of persin (IC_{50} ~55 μmol/L) compared with T-47D and MCF-7 cells (IC_{50} ~6.9 μmol/L).

Flow cytometric analysis of propidium iodide−stained nuclei was used to detect and quantitate the apoptotic process in T-47D and MDA-MB-231 cells. Figure 4B shows the apoptotic (pre-G_1) fraction in persin-treated cells as a percentage of untreated controls. T-47D cells showed a significant induction of apoptosis following persin treatment compared with untreated controls. This effect was not observed in MDA-MB-231 cells. MCF-7 cells do not express caspase-3 and, consequently, do not display some of the

morphologic features of apoptosis associated with DNA fragmentation. However, the apoptotic process can be quantitated in these cells by determining the abundance of the M30 epitope, which is present only on caspase-cleaved cytokeratin 18 (13). Treated cells were incubated with M30 CytoDEATH monoclonal antibody before flow cytometric analysis. Figure 4C shows that there was a significant increase in the M30-positive (apoptotic) population 24 hours following treatment of MCF-7 cells with persin.

We examined the involvement of caspase activation in persin-induced apoptosis using the caspase-8- and caspase-9-specific inhibitors z-IETD-fmk and z-LEHD-fmk, respectively. Incubation of T-47D cells with either inhibitor significantly inhibited the level of persin-induced apoptosis (Fig. 4D). This suggests that blocking activation of either caspase-8 or caspase-9 can attenuate persin-induced apoptosis.

Bcl-2 Overexpression Does Not Fully Protect against Persin-Induced Apoptosis

The intrinsic apoptotic pathway centers on the release of mitochondrial cytochrome c and Smac/DIABLO into the cytoplasm and the subsequent activation of caspase-9. To further investigate the intracellular mechanism of persin-induced apoptosis, we determined the effects of treatment on the release of these mitochondrial components. Figure 5A shows that in sensitive cells, persin treatment was associated with a rapid (within 8 hours) release of cytochrome c and Smac/DIABLO into the cytoplasmic compartment. This was not observed in the resistant MDA-MB-231 cell line.

To determine whether this phenomenon was initiated via changes in expression of Bcl-2 proteins, we examined the expression of both proapoptotic (Bax, Bad, Bak, and Bcl-x_S) and antiapoptotic (Bcl-2 and Bcl-x_L) members of the Bcl-2 family following persin treatment. Figure 5B shows that no significant modulations in expression of these proteins were observed following persin treatment up to 24 hours, compared with untreated controls. T-47D cells do not express detectable levels of Bcl-2 protein (14).

To exclude the possibility that persin may influence the interactions of proapoptotic and antiapoptotic Bcl-2-like
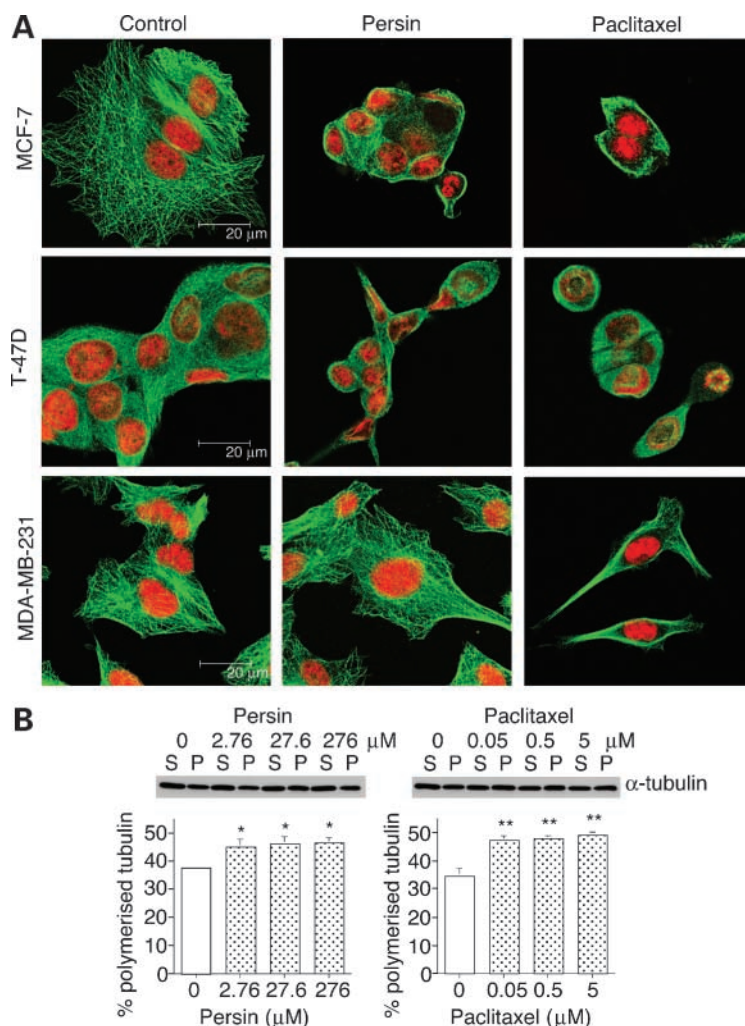

Figure 3. Persin affects microtubule morphology. **A,** cells were grown on sterile glass slides and treated with 13.8 μmol/L persin or 10 μmol/L paclitaxel for 16 h. Microtubules were detected by α-tubulin staining (*green*) and nuclei were detected with the fluorescent DNA dye 4′,6-diamidino-2-phenylindole (*red*) and visualized by confocal microscopy. Representative images from at least three independent experiments. **B,** MCF-7 cells were treated with persin or paclitaxel for 1 h, then soluble (*S*) and polymerized (*P*) pools of tubulin were separated and relative amounts determined by immunoblotting. The percent polymerized tubulin was calculated by dividing the polymerized fraction by the total polymerized and soluble fractions. Immunoblots are representative of three independent experiments. *Columns,* mean of triplicate wells from three independent experiments; *bars,* SE. *, $P < 0.05$; **, $P < 0.02$, treated cells versus untreated controls.
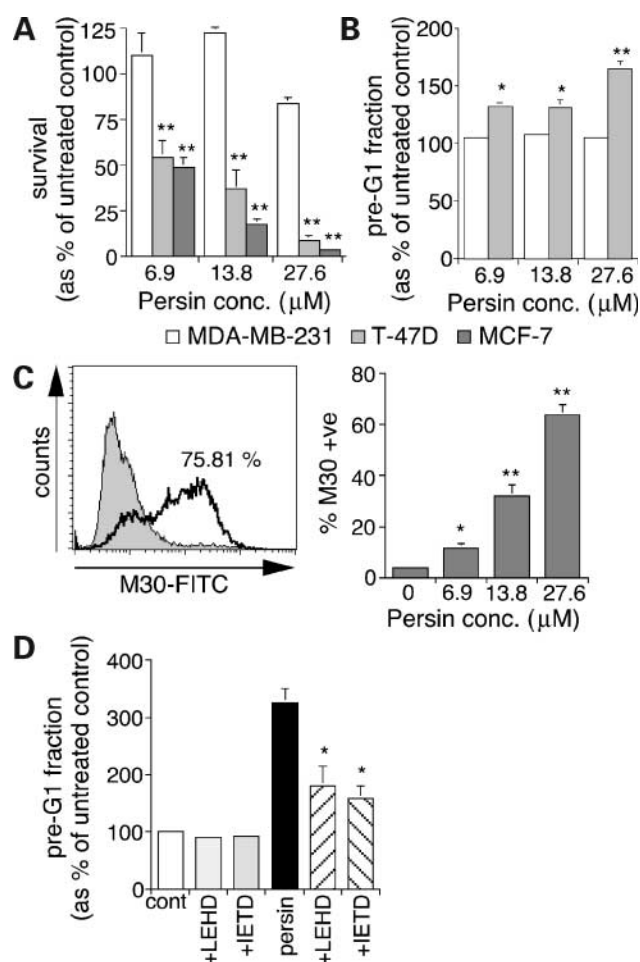
Figure 4. Effect of persin treatment on the survival of human breast cancer cells. **A,** survival was measured 14 d posttreatment by clonogenic assay. *Columns,* mean of triplicate wells from three independent experiments; *bars,* SE. **B,** T-47D and MDA-MB-231 cells were analyzed for DNA fragmentation (pre-G$_1$ fraction) by flow cytometry following persin treatment. *Columns,* mean of triplicate wells from three independent experiments; *bars,* SE. *, $P < 0.05$; **, $P < 0.001$, persin-treated cells versus untreated controls. **C,** MCF-7 cells were incubated in the presence (*unshaded area*) or absence (*shaded area*) of persin for 24 h, then attached and floating populations were analyzed for M30-FITC positivity by flow cytometry. *Columns,* mean of triplicate wells from three independent experiments; *bars,* SE. *, $P < 0.001$; **, $P < 0.0001$, persin-treated cells versus untreated controls. **D,** T-47D cells were treated with 27.6 μmol/L persin in the presence or absence of caspase-8-specific (z-IETD-fmk) or caspase-9-specific (z-LEHD-fmk) inhibitors. Apoptosis was detected by flow cytometry. *Columns,* mean of triplicate wells from three independent experiments; *bars,* SE. *, $P < 0.05$, persin- and inhibitor-treated cells versus persin-treated cells.

proteins without altering expression levels, we determined the effects of Bcl-2 overexpression on persin-induced apoptosis. We isolated clones of MCF-7 and T-47D cells stably overexpressing human Bcl-2 cDNA and vector alone controls. Figure 5C illustrates the long-term survival of persin-treated T-47D cells compared with untreated controls. Overexpression of Bcl-2 protein significantly increased the long-term survival of persin-treated cells

compared with the vector controls at concentrations of 6.9 and 13.8 μmol/L. However, the percentage surviving was still only $\sim$60% and 45% at the two concentrations, respectively, suggesting that Bcl-2 does not fully protect sensitive cells against persin-induced apoptosis. Similar results were obtained in MCF-7 cells (data not shown). Figure 5D shows that overexpression of Bcl-2 did not affect the persin-induced activation of caspase-9 when compared with vector controls.

Persin-Induced Apoptosis Is Dependent on Bim Expression

The BH3-only protein Bim links microtubule damage with the induction of apoptosis. We examined the expression of Bim$_{EL}$, Bim$_L$, and Bim$_S$ in response to persin treatment. Figure 6A shows that there is a differential expression of the Bim isoforms in sensitive and resistant cell lines, with the resistant MDA-MB-231 cells expressing very low levels of Bim$_{EL}$ and undetectable levels of Bim$_L$ and Bim$_S$. In MCF-7 and T-47D cells, a consistent increase in Bim expression was seen with persin treatment up to 24 hours.

We determined the dependence of persin-induced apoptosis on Bim expression using Bim-specific siRNA. MCF-7 cells were treated with either nontargeting siRNA or with Bim-specific siRNAs (#6 and #7) and analyzed for Bim expression by immunoblot. Figure 6B shows that treatment with either of the Bim-specific siRNAs significantly reduced expression of the Bim isoforms compared with untreated whole-cell lysates and the nontargeting control. Figure 6B shows that, consistent with Figure 5A, persin treatment induces a release of cytochrome *c* and Smac/DIABLO into the cytoplasm, but this is significantly attenuated in the presence of Bim siRNAs. Persin-induced apoptosis, as assessed by M30-FITC positivity, was also significantly reduced in the presence of Bim siRNA compared with nontargeting siRNA controls (Fig. 6B).

An important upstream regulator of Bim is the stress kinase JNK. Levels of JNK activation were determined by phospho-specific immunoblot. Figure 6C shows that there was a rapid phosphorylation of JNK (within 30 minutes) in response to persin in MCF-7 cells. This activation was sustained for 2 to 3 hours, and then returned to basal levels.

We further examined the relationship between Bim expression and response to persin in a panel of human breast cancer cell lines (Table 1). Cells were examined for their cytostatic and cytotoxic responsiveness to persin, the expression of estrogen receptor, p53, and Bim isoforms, and the presence of microtubule bundling following persin treatment. Whereas response to persin was independent of the estrogen receptor and p53 status of the cells, it was associated with expression of the Bim$_{EL}$ isoform and the presence of microtubule bundling. For example, SK-Br3 cells (estrogen receptor negative) express comparable levels of the Bim isoforms to MCF-7 cells and exhibit a similar level of sensitivity to persin, whereas Hs 578.T cells (estrogen receptor negative) do not express detectable levels of Bim and are resistant to persin.

Discussion

Over recent years, there has been considerable interest in exploiting the cytostatic and cytotoxic effects of phytochemicals in the treatment of human cancers. Here we describe the characterization of a novel plant toxin, persin. Previous studies using a lactating mouse model isolated persin as the bioactive component of avocado leaves causing mammary-specific necrosis and apoptosis. Persin is a derivative of glyceride with strong structural homology to linoleic acid. Here we show that dosing of lactating dams with persin results in severe necrosis and/or apoptosis of the mammary gland, consequential inhibition of milk flow, and decreased pup weight. This activity in the mammary gland suggests that persin or related compounds could be developed as selective agents for the treatment of breast cancer. We therefore went on to further delineate the mechanism of action of persin in human breast cancer cells.

Three human breast cancer cell lines, T-47D, MCF-7, and MDA-MB-231, were examined for their response to persin using cell proliferation assays. T-47D and MCF-7 were exquisitely sensitive to the inhibitory effects of persin whereas MDA-MB-231 cells were relatively resistant. This cell line–specific inhibition of proliferation led us to examine the effects of persin on cell cycle progression. Persin treatment was associated with a significant accumulation of cells with a G_2-M phase DNA content, consistent with a cell cycle arrest. These effects on cell cycle progression were confirmed by analysis of cyclin expression, showing a significant decrease in expression of cyclins A, D1, and B.

The G_2-M arrest observed in persin-treated cells has similarities to that induced by microtubule inhibitors such as the taxanes, leading us to hypothesize that persin may exhibit a similar mode of action. The taxanes mediate their cytotoxicity by binding to tubulin and stabilizing the microtubules, resulting in the formation of microtubule bundles with subsequent mitotic arrest and apoptosis (2). Morphologic examination of microtubules in sensitive cells
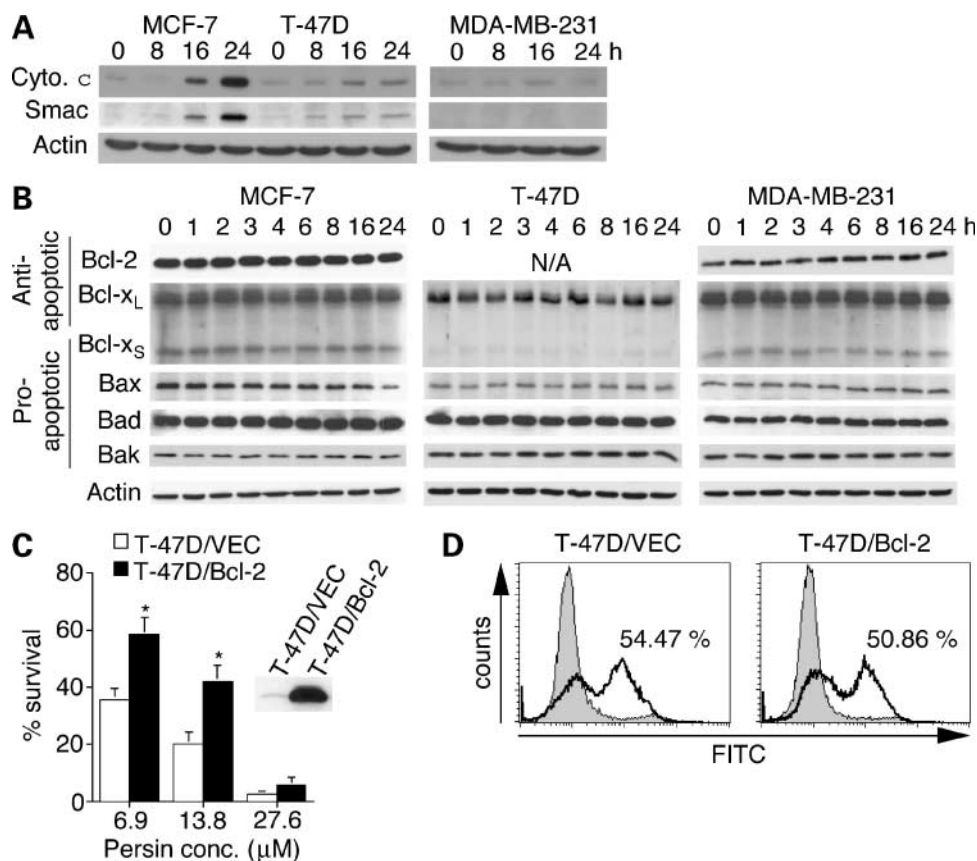

Figure 5. Involvement of Bcl-2 in persin action. **A,** persin treatment is associated with release of cytochrome *c* and Smac/DIABLO from mitochondria. Cells were treated with 27.6 μmol/L persin for various time periods, then cytoplasmic extracts were prepared and immunoblotted for cytochrome *c* and Smac/DIABLO expression. Expression of actin was used as a loading control. Representative immunoblots from two independent experiments. **B,** cells were treated with 27.6 μmol/L persin and analyzed for expression of Bax, Bad, Bak, Bcl-x$_S$ (proapoptotic), Bcl-2, and Bcl-x$_L$ (antiapoptotic) proteins by immunoblot at time points up to 24 h. T-47D cells do not express detectable levels of Bcl-2. Expression of actin was used as a loading control. Representative immunoblots from two independent experiments. **C,** the survival of T-47D clones overexpressing *bcl-2* cDNA or vector controls was analyzed by clonogenic assay. *Columns,* mean of triplicate wells from three independent experiments; *bars,* SE. *, $P < 0.05$, T-47D/Bcl-2 versus T-47D/VEC. **D,** T-47D/VEC and T-47D/Bcl-2 cells were incubated with (*black lines*) or without (*shaded area*) 27.6 μmol/L persin for 24 h, then cells were stained with carboxyfluorescein-labeled caspase-9 inhibitor, FAM-LETD-fmk, and analyzed for caspase-9 activation by flow cytometry.
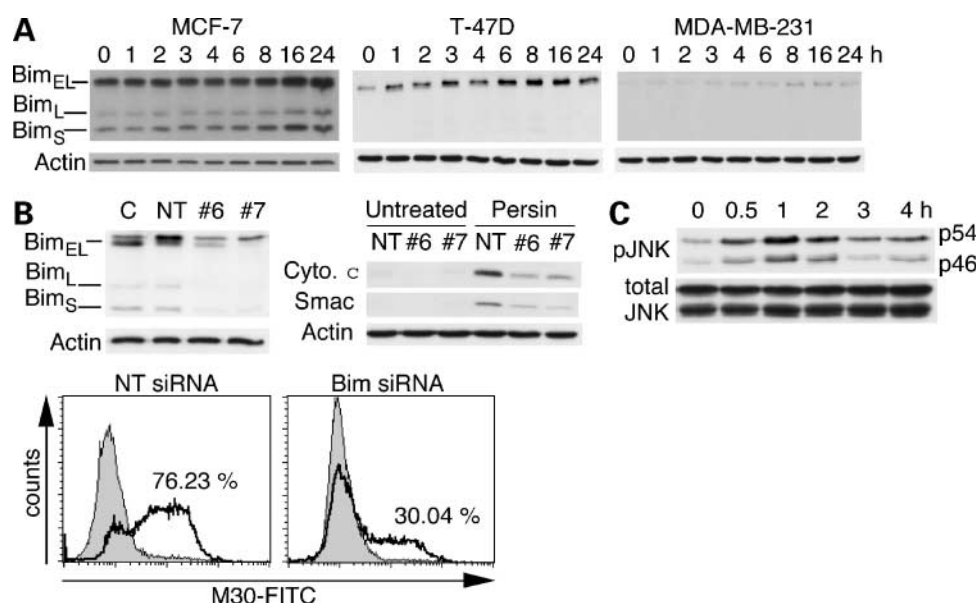
Figure 6. Persin-induced apoptosis is dependent on Bim expression. **A,** cells were treated with 27.6 μmol/L persin then analyzed for expression of Bim_{EL}, Bim_L, and Bim_S by immunoblot. Actin was used as a loading control. **B,** *top left,* MCF-7 cells were treated with Bim-specific siRNAs (*#6* and *#7*) or nontargeting control (*NT*) for 24 h, then Bim expression was determined by immunoblot and compared with whole-cell lysates (*C*) from untreated cells. *Top right,* MCF-7 cells were treated with siRNAs as described above in the presence or absence of 27.6 μmol/L persin for 24 h, then cytoplasmic extracts were analyzed for cytochrome *c* and Smac/DIABLO expression by immunoblot. *Bottom,* MCF-7 cells treated with siRNAs in the presence (*unshaded area*) or absence (*shaded area*) of 27.6 μmol/L persin for 24 h were incubated with M30-FITC and analyzed by flow cytometry. **C,** levels of phospho-JNK in persin-treated MCF-7 cells. Cells were treated with 10 mg/mL persin for the indicated time periods, then levels of phospho-JNK were determined by immunoblotting. Total JNK expression was used as a loading control. Representative blots from three independent experiments.

showed that persin induced bundling of microtubules, similar to that seen with paclitaxel. There is also evidence to suggest that, like paclitaxel, persin can induce polymerization of tubulin, with the lowest dose of 2.76 μmol/L seeming to produce maximal effect. Whether persin interacts directly with tubulin to cause these effects has not yet been examined. Whereas persin and paclitaxel seem to elicit similar effects on tubulin polymerization, the effective dose of persin is 1 to 2 orders of magnitudes higher than that observed for paclitaxel (2.76 and

0.05 μmol/L, respectively). This may reflect differences in the solubility and cellular uptake of these compounds, or, if direct binding to tubulin is involved, a lower affinity for tubulin. Alternatively, it is known that persin becomes active orally by metabolic conversion in the gut (6); thus, it is plausible that the form of the compound used in our *in vitro* studies does not have maximal potency.

Interestingly, other microtubule-targeting agents, such as colchicine and the *Vinca* alkaloids, affect the lactating mammary gland, resulting in the inhibition of milk

Table 1. Response of breast cancer cells to the cytostatic and cytotoxic effects of persin

Cell line	Estrogen receptor status	p53 status	Bim status*	Response to persin		
				Growth inhibition[†]	Apoptosis[‡]	Microtubule bundling
MCF-7	+	wt	+++	+++	+++	+
T-47D	+	mut	+--	++	+++	+
MDA-MB-231	−	mut	---	−	−	−
MDA-MB-157	−	mut	+--	++	++	+
MDA-MB-361	+	wt	+--	++	++	+
Hs 578.T	−	mut	---	+	−	−
SK-Br3	−	mut	+++	++	+++	+

NOTE: Cell lines were treated with 27.6 μmol/L of persin for 24 hours (growth inhibition and apoptosis) or 13.8 μmol/L for 16 hours (microtubule bundling). Estrogen receptor, p53, and Bim status were determined by immunoblotting.
*Bim_{EL}, Bim_L, and Bim_S.
[†] 3-(4,5-Dimethylthiazol-2-yl)-2,5-diphenyltetrazolium bromide assay.
[‡] M30 positivity.

secretion from secretory acinar cells (reviewed in ref. 15), with some evidence that the maintenance of microtubule integrity is required for prolactin function. However, unlike persin, there are no data showing that these agents induce proapoptotic changes in the acinar epithelium, suggesting that persin may directly engage an apoptotic pathway in breast epithelium that is distinct from its effects on tubulin, a hypothesis that is supported by the differential sensitivity of MDA-MB-231 cells to persin and paclitaxel.

Further analysis of the mechanism of action of persin showed that cytotoxic effects also contribute to the persin-induced growth inhibition seen in sensitive cells. Persin treatment significantly reduced the survival of T-47D and MCF-7 cells, and further studies showed that this was due to an induction of caspase-dependent apoptosis. Interestingly, inhibitors of the apical caspases of both extrinsic and intrinsic apoptotic pathways abrogated persin-induced cell death. This may reflect the cross-talk between these pathways, acting to amplify the apoptotic signal downstream of the initiating stimuli. For example, death receptor–independent activation of caspase-8 occurs downstream of mitochondrial cytochrome c release and caspase-9 activation in MCF-7 cells in response to staurosporine (16). Thus, in persin-induced apoptosis, caspase-9 may be the initiating caspase that subsequently activates caspase-8, and z-IETD-fmk at the concentrations used in this study may delay rather than prevent cell death.

Investigation of the molecular mechanism of persin-induced apoptosis showed a rapid efflux of cytosolic cytochrome c and Smac/DIABLO following treatment. However, no significant differences in proapoptotic or antiapoptotic members of the Bcl-2 family were observed, suggesting that persin is not regulating an intrinsic apoptotic pathway by modulating Bcl-2 family protein expression in sensitive cells. This was further confirmed with cells overexpressing Bcl-2, wherein persin-induced apoptosis was reduced but not fully abrogated, suggesting the triggering of a parallel Bcl-2-independent apoptotic cascade. Alternatively, these data could reflect a titration effect wherein the level of Bcl-2 overexpression is sufficient to inhibit partial, but not full, mobilization of a proapoptotic Bcl-2 family protein, such as Bim.

The mechanisms linking the disruption of microtubule integrity to the initiation of apoptosis are not entirely clear, although it has been postulated that the induction of a prolonged mitotic arrest drives cells into apoptosis via a Bcl-2-dependent pathway (3). However, whereas there have been reports of Bcl-2 overexpression blocking paclitaxel-induced apoptosis *in vitro*, this may be dose dependent, and clinical studies suggest that the response to paclitaxel in breast cancer is not influenced by Bcl-2 expression (17).

The proapoptotic BH3-only protein Bim also mediates the induction of apoptosis following cytoskeletal perturbations (18). In healthy cells, Bim localizes to microtubules via binding to the light chain of the dynein motor complex (19). Potential upstream mediators of Bim include the FoxO3 family of transcriptional regulators (20) and the stress kinase JNK (21), and our studies have shown that the latter is activated rapidly following persin treatment. Activated JNK not only increases expression of Bim but can also induce its dissociation from the dynein motor complex by phosphorylation (21). Once dissociated from the cytoskeleton, Bim translocates to the mitochondria where it binds to Bcl-2 and Bcl-x_L and sequesters them from proapoptotic proteins such as Bax and Bak. The latter then initiate the efflux of cytochrome c and Smac/DIABLO from the mitochondria. There is also evidence to suggest that Bim may directly activate Bax/Bak by inducing a conformational change (22, 23). Thus, although we did not observe significant changes in the expression of these proteins following persin treatment, the up-regulation of Bim could initiate a critical change in the balance of active Bcl-2-like proteins leading to the triggering of mitochondrial changes. Consistent with its role as a sensor of microtubule integrity, Bim expression also modulates the response to paclitaxel in MCF-7 cells (20) and in epithelial tumor models *in vivo* (24).

We extended these studies to a panel of human breast cancer cell lines and observed that the majority of cell lines examined were responsive to the cytostatic [assessed by 3-(4,5-dimethylthiazol-2-yl)-2,5-diphenyltetrazolium bromide assay] and cytotoxic (assessed by M30-FITC positivity) effects of persin (Table 1). Sensitivity to persin was independent of the p53 and estrogen receptor status of the cells, which has particular relevance to the treatment of breast cancer where both have been shown to be critical regulators of therapeutic responsiveness. Furthermore, sensitivity to the apoptotic effects of persin was associated with the expression of Bim, particularly the Bim$_{EL}$ isoform, and the induction of microtubule perturbations (Table 1). These data, together with our observation that persin-induced apoptosis is abrogated following specific knockdown of Bim expression, suggest that cell death may proceed via a Bim-dependent mechanism. Thus, the very low levels of Bim expressed by MDA-MB-231 may mediate their resistance to persin-induced apoptosis. However, MDA-MB-231 cells were also resistant to the cytostatic effects of persin, indicating that additional resistance mechanisms may exist, or that the lack of response is mediated proximal to the initiating cascades, possibly at the level of cellular uptake of the compound. Further studies with resistant cell lines should provide more insight into the mechanisms of persin uptake, action, and resistance.

Thus, we propose that persin-induced apoptosis is mediated via the activation of Bim. This may occur either directly through the effects of persin on microtubule integrity or through the convergence of multiple apoptotic and antiproliferative signals. Once activated, Bim shifts the equilibrium of active Bcl-2 proteins towards an apoptotic phenotype, resulting in the release of cytochrome c and Smac/DIABLO and the initiation of a caspase activation cascade.

In summary, we have described the potent cytostatic and cytotoxic effects of a novel plant toxin, persin, in a panel of

human breast cancer cell lines. Sensitivity to the apoptotic effects of persin is associated with the expression of Bim and changes to tubulin indicative of increased polymerization. Furthermore, response to persin is independent of the estrogen receptor, p53, and Bcl-2 status of the cells, emphasizing its potential as a clinically relevant therapeutic for refractory disease. These results provide support for persin to be further evaluated as a single-agent or combination chemotherapeutic for cancers of the breast and, potentially, other organs.

References

1. Butt AJ, McNeil CM, Musgrove EA, Sutherland RL. Downstream targets of growth factor and oestrogen signalling and endocrine resistance: the potential roles of c-Myc, cyclin D1 and cyclin E. Endocr Relat Cancer 2005;12:S47 – 59.

2. Altmann K-H. Microtubule-stabilizing agents: a growing class of important anticancer drugs. Curr Opin Chem Biol 2001;5:424 – 31.

3. Mollinedo F, Gajate C. Microtubules, microtubule-interfering agents and apoptosis. Apoptosis 2003;8:413 – 50.

4. Kingsbury JM. Poisonous plants of the United States and Canada. New Jersey: Prentice-Hall; 1964. p. 124 – 5.

5. Sani Y, Seawright AA, Ng JC, O'Brien GP, Oelrichs PB. The toxicity of avocado leaves for the heart and lactating mammary gland in the mouse. Hum Exp Toxicol 1994;13:189.

6. Oelrichs PB, Ng JC, Seawright AA, Ward A, Schaffeler L, MacLeod JK. Isolation and identification of a compound from avocado (*Persea americana*) leaves which causes necrosis of the acinar epithelium of the lactating mammary gland and the myocardium. J Nat Toxins 1995;3: 344 – 9.

7. Rodriguez-Saona C, Trumble JT. Biologically active aliphatic acetogenins from specialized idioblast oil cells. Curr Org Chem 2000;4:1249 – 60.

8. Ip C, Dong Y, Ip MM, et al. Conjugated linoleic acid isomers and mammary cancer prevention. Nutr Cancer 2002;43:52 – 8.

9. Menendez JA, del Mar Barbacid M, Montero S, et al. Effects of γ-linolenic acid and oleic acid on paclitaxel cytotoxicity in human breast cancer cells. Eur J Cancer 2001;37:402 – 13.

10. Butt AJ, Dickson KA, Jambazov S, Baxter RC. Enhancement of tumor necrosis factor-α-induced growth inhibition by insulin-like growth factor-binding protein-5 (IGFBP-5), but not IGFBP-3 in human breast cancer cells. Endocrinology 2005;146:3113 – 22.

11. Heibein JA, Barry M, Motyka B, Bleackley RC. Granzyme B-induced loss of mitochondrial inner membrane potential and cytochrome *c* release are caspase independent. J Immunol 1999;163:4683 – 93.

12. Don S, Verrills NM, Liaw T, et al. Neuronal-associated microtubule proteins class III β-tubulin and MAP2c in neuroblastoma: role in resistance to microtubule-targeted drugs. Mol Cancer Ther 2004;3:1137 – 46.

13. Hostanska K, Nisslein T, Freudenstein J, Reichling J, Saller R. *Cimicifuga racemosa* extract inhibits proliferation of estrogen receptor-positive and negative human breast carcinoma cell lines by induction of apoptosis. Breast Cancer Res Treat 2004;84:151 – 60.

14. Runnebaum IB, Nagarajan M, Bowman M, Soto D, Sukumar S. Mutations in p53 as potential molecular markers for human breast cancer. Proc Natl Acad Sci U S A 1991;88:10657 – 61.

15. Craigmill AL, Seawright AA, Mattila T, Frost AJ. Pathological changes in the mammary gland and biochemical changes in milk of the goat following oral dosing with leaf of the avocado (*Persea americana*). Aust Vet J 1989;66:206 – 11.

16. Deng Y, Ren X, Yang L, Lin Y, Wu X. A JNK-dependent pathway is required for TNFα-induced apoptosis. Cell 2003;115:61 – 70.

17. Poelman SM, Adeyanju MO, Robertson MA, et al. Human breast cancer susceptibility to paclitaxel therapy is independent of Bcl-2 expression. Clin Cancer Res 2000;6:4043 – 8.

18. Strasser A, Puthalakath H, Bouillet P, et al. The role of Bim, a proapoptotic BH3-only member of the Bcl-2 family, in cell-death control. Ann N Y Acad Sci 2000;917:541 – 8.

19. Puthalakath H, Huang DCS, O'Reilly LA, King SM, Strasser A. The proapoptotic activity of the Bcl-2 family member Bim is regulated by interaction with the dynein motor complex. Mol Cell 1999;3:287 – 96.

20. Sunters A, Fernandez de Mattos S, Stahl M, et al. Fox03a transcriptional regulation of Bim controls apoptosis in paclitaxel-treated breast cancer cell lines. J Biol Chem 2003;278:49795 – 805.

21. Lei K, Davis RJ. JNK phosphorylation of Bim-related members of the Bcl2 family induces Bax-dependent apoptosis. Proc Natl Acad Sci U S A 2003;100:2432 – 7.

22. Kuwana T, Bouchier-Hayes L, Chipuk JE, et al. BH3 domains of BH3-only proteins differentially regulate Bax-mediated mitochondrial membrane permeabilization both directly and indirectly. Mol Cell 2005; 17:525 – 35.

23. Marani M, Tenev T, Hancock D, Downward J, Lemoine NR. Identification of novel isoforms of the BH3 domain protein Bim which directly activate Bax to trigger apoptosis. Mol Cell Biol 2002;22: 3577 – 89.

24. Tan T-T, Degenhardt K, Nelson DA, et al. Key roles of BIM-driven apoptosis in epithelial tumors and rational chemotherapy. Cancer Cell 2005;7:227 – 38.